PERGAMON

International Journal of Heat and Mass Transfer 43 (2000) 127–138

International Journal of HEAT and MASS TRANSFER

www.elsevier.com/locate/ijhmt

Energy transfer between an aerosol particle and gas at high temperature ratios in the Knudsen transition regime

A.V. Filippov*, D.E. Rosner

Department of Chemical Engineering, Yale University, High Temperature Chemical Reaction Engineering (HTCRE) Laboratory, New Haven, CT 06520-8286, USA

Received 15 July 1998; received in revised form 26 March 1999

Abstract

Motivated by the Laser-Induced Incandescence (LII) technique for in situ sizing of submicron aerosols, non-continuum heat transfer between an isolated, motionless, highly overheated spherical particle and its cooler surrounding gas is studied using the Direct Monte Carlo Simulation (DSMC) technique for the 'calibration' case of a monatomic, hard-sphere gas. We find that our numerical DSMC results are adequately described by a variable property extension of Fuchs' two-layer theory, whereas other interpolation formulae fail in the Knudsen transition regime when the particle/gas temperature ratio is large. On this basis, tractable equations are provided which will permit accurate estimates of the transition regime heat transfer coefficient for a polyatomic ideal gas with arbitrary temperature-dependent heat capacity and Fourier conductivity.

1. Introduction

Energy exchange between a spherical body and a quiescent gas in the Knudsen transition regime is a classical problem in kinetic theory of gases [1]. In both the free-molecular and continuum limiting cases, this problem admits quasi-steady analytical solutions. There are also simple interpolation formulae, which cover the intermediate regime [2] and agree well with available experimental data in the near-isothermal limit.

Usually, it is assumed that the particle–gas temperature difference ΔT is small compared to the gas temperature T_g, which allows linearization with respect to the small parameter $\Delta T/T_g$, simplifying such problems considerably. However, this assumption cannot be made in many important cases, e.g., when aerosol particles are suddenly heated by a powerful laser pulse. For example, in probing aerosols by the laser-induced incandescence method (LII) (see, e.g., [3]), the particle–carrier gas temperature difference may exceed the gas temperature by even more than one decade for aerosols originally at room temperature. In applications of LII analysis to aerosol characterization in flames [4], typical values of $\Delta T/T_g$ are between 1 and 3. Large differences between particle and gas temperatures are also encountered in thermal plasma processing, when relatively cool particles are injected into plasmas having temperature of several thousand Kelvins. Xi and Ping [5] have found an analytical solution for the heat transfer between a moving particle and thermal plasma in free-molecular regime, while Lee et al. [6] used the Fuchs theory to calculate the particle–plasma heat flux in the transition regime of intermediate Knudsen numbers.

For moderate and large ratios $\Delta T/T_g$, linearization cannot be justified and available interpolation for-

* Corresponding author. Tel.: +1-203-432-4380; fax: +1-203-432-7232.

E-mail address: andrey.filippov@yale.edu (A.V. Filippov)

0017-9310/00/$ - see front matter
PII: S0017-9310(99)00113-1

Nomenclature

a	particle radius
$\bar{c}$	mean thermal speed of the gas molecules
c_p	specific heat capacity of the particle
c_v	specific heat capacity of the gas at constant volume
f	velocity distribution function of molecules
f_0	Maxwellian equilibrium velocity distribution
F	function describing variable property effects
l	mean free path of the gas molecules
L	geometric diameter of the aggregate
k	heat conductivity coefficient
k_B	Boltzmann constant
Kn	Knudsen number
m_g	mass of a gas molecule
$\boldsymbol{n}$	external normal vector
n_m	number density of molecules
N	number of spherules in an agglomerate
Nu_h	Nusselt number
p	gas pressure
$\dot{q}$	heat transfer rate
r	distance from the particle center
R	gas/solid scattering kernel function
R_{eq}	equivalent radius of the aggregate (for heat transfer)
T	temperature
U_I	internal energy per gas molecule
$\boldsymbol{v}$	velocity vector of the gas molecule
$\boldsymbol{v}'$	velocity vector of the incident molecules
$\boldsymbol{v}_*$	dimensionless velocity of the gas molecule.

Greek symbols

α	energy accommodation coefficient (gas/solid interface)
γ	adiabatic constant of the ideal gas, $[(k_B/m_g)+c_v]/c_v$
γ^*	average value of adiabatic constant [Eq. (6)]
δ	thickness of the boundary layer in Fuchs and DSMC models
δ_D	Dirac's delta function
ΔT	particle–gas temperature difference, T_p-T_g
ζ	constant parameter in formula (21)
Θ	temperature ratio, T_p/T_g
Λ_i	auxiliary dimensionless parameters in Eq. (16), $i = 1, 2$
ξ	auxiliary factor in the interpolation formula (21)
ρ	mass density
τ_{eq}	gas equilibration time
$\tau_{p,h}$	characteristic particle cooling time
Φ	heat flux potential
ω	exponent in the power law for heat conductivity coefficient.

Subscripts

c	continuum limit
c,l	linearized in the continuum limit
f	free-molecular limit
g	background gas in unperturbed state
h	heat transfer
i	incident gas molecules
ncp	non-constant (variable) property
p	particle
r	radial component of a vector
ref	reference value
δ	corresponding to the limiting sphere at $r=\delta$.

mulae must be corrected to account for appreciable temperature differences. To analyze the altered particle–gas heat transfer laws under such highly non-equilibrium conditions, at least in the absence of sublimation or chemical reaction, we have applied a direct Monte Carlo simulation method (DSMC of Bird, [7]), already successfully tested on a class of transition regime gas–solid enclosure heat transfer problems by Papadopoulos and Rosner [8]. The background gas molecules are modeled as hard spheres in the region adjacent to the motionless spherical particle, while, at several mean free paths from the surface, the DSMC solution is matched to the analytical, variable-property continuum solution in the infinite 'outer' region. Matching of the two solutions is carried out iteratively, with good convergence. Our strategy is to calculate the heat transfer rates using the DSMC method over a wide range of Knudsen numbers and accommodation coefficients and compare the results with predictions of known interpolation formulae. Only the formulae passing such a test are likely to be adequate in calculating the heat transfer rates under real non-equilibrium conditions.

The numerical calculations have shown that only a generalized Fuchs' two-layer model of the variable property thermal boundary layer adequately predicts the heat transfer rates at high particle/gas temperature ratios. We conclude with a discussion of extensions in progress, gas/surface energy accommodation under such conditions [9], and the implications of these new

results for accurate inferences of particle size using the LII method.

2. Heat transfer in limiting cases

2.1. Free-molecular regime

Consider a spherical particle having a temperature T_p in a gas which has a temperature T_g far from the particle. Suppose that the particle radius a is much smaller than the mean free path of gas molecules l_g, so that the Knudsen number $Kn = l_g/a$ is large. Then the energy flow rate $\dot{q}_i$ to

$$\dot{q}_i = \pi a^2 n_g \bar{c}(2k_B T_g + U_I(T_g)) \tag{1}$$

the particle brought by the incident molecules, is given by the formula (see, e.g., Refs. [10,11])

$$\bar{c} = \sqrt{\frac{8k_B T_g}{\pi m_g}} \tag{2}$$

where, for any reference temperature T_{ref} (including 298.16 K),

$$U_I(T) \equiv \int_{T_{ref}}^{T} m_g c_v(T)\,dT - \frac{3}{2}k_B(T - T_{ref}) \tag{3}$$

and c_v is the specific heat capacity of the gas, n_g, c and m_g are the concentration, the mean speed and the mass of the gas molecules, k_B is the Boltzmann constant and U_I is the internal (other than translational) energy per gas molecule. Usually, the energy flux from the particle is calculated assuming partial accommodation of energy on the particle surface. Under such an assumption, Eqs. (1) and (3) yield the following formula for the net energy transfer rate between the particle and the gas q_f:

$$\dot{q}_f = \alpha\pi a^2 n_g \bar{c} k_B \left(\frac{1}{2}(T_p - T_g) + \int_{T_g}^{T_p} \frac{dT}{\gamma - 1}\right) \tag{4}$$

where α is the energy accommodation coefficient and γ is the adiabatic exponent (ratio of the gas specific heats at constant pressure and volume, respectively). It is assumed that in the case of complete accommodation ($\alpha = 1$), reflection of molecules at the particle surface is diffuse. Generally, the accommodation coefficient depends on the nature of gas and particle surface, as well as their temperatures, as discussed by Burke and Hollenbach [12].

Eq. (4) can be formally simplified by introducing an appropriate average value γ^* of the adiabatic constant on the interval $[T_g, T_p]$:

$$\dot{q}_f = \alpha\pi a^2 \frac{p_g \bar{c}}{2}\left(\frac{\gamma^* + 1}{\gamma^* - 1}\right)(\Theta - 1) \tag{5}$$

where

$$\frac{1}{\gamma^* - 1} \equiv \frac{1}{T_p - T_g}\int_{T_g}^{T_p} \frac{dT}{\gamma - 1} \tag{6}$$

and Θ is the temperature ratio T_p/T_g. For polyatomic gases and for monatomic gases with electronic excitation, the temperature variation of γ may be especially important and can lead to significant variation of the heat transfer rates. Consider, for example, the particle heated up to the temperature $T_p = 3500$ K in nitrogen with temperature $T_g = 1500$ K. Then, the calculation based on Eq. (6) and heat capacity values of JANAF Tables [13] yields $\gamma^* = 1.3$ and the factor $(\gamma^* + 1)/(\gamma^* - 1) = 7.8$ in Eq. (5). At room temperature, $\gamma = 1.4$, and this ratio is equal to 6.

The last (diatomic) example shows the importance of accounting for internal degrees-of-freedom in energy transfer calculations. If we had neglected the internal rotational and vibrational energy of the gas and assume $\gamma = 5/3$, $(\gamma^* + 1)/(\gamma^* - 1) = 4$, this would result in almost 50% underestimate in the heat flux from the particle. The corresponding error for a polyatomic gas would be even larger.

2.2. Continuum regime

In the continuum regime the heat transfer between the particle and the gas is diffusion-controlled and depends on the gas temperature distribution near the particle. Solution of the stationary continuum heat transfer equations in the infinite quiescent region outside a spherical particle yields

$$\dot{q}_c = 4\pi a[\Phi(T_p) - \Phi(T_g)] \tag{7}$$

where

$$\Phi(T) = \int_{T_{ref}}^{T} k(T)\,dT \tag{8}$$

Here $k(T)$ is the Fourier heat conductivity coefficient of the gas and Φ is called the heat flux 'potential' (see, e.g., Rosner [14]). If the ratio $\Delta T/T_g$ is small, Eq. (7) can be linearized to yield a commonly used equation:

$$\dot{q}_{c,1} = 4\pi a k(T_g)(T_p - T_g) \tag{9}$$

In many cases the dependence of the gas heat conductivity on the gas temperature may be approximated by a power law:

$$k(T) = k(T_g)\left(\frac{T}{T_g}\right)^{\omega} \tag{10}$$

which leads to the following equation:

$$\dot{q}_c = \frac{4\pi a k(T_g) T_g}{\omega + 1}(\Theta^{\omega+1} - 1) \tag{11}$$

where ω is a constant parameter. Typical values of the exponent ω for real gases lie between 0.6 and 0.9, while for the hard sphere intermolecular potential $\omega = 1/2$. For moderate ratios $\Delta T/T_g$ Eq. (11) for heat transfer rate can exceed the values predicted by its linearized version (9) considerably, according to the equation

$$\frac{\dot{q}_c}{\dot{q}_{c,1}} = \frac{1}{(\omega+1)} \frac{(\Theta^{\omega+1} - 1)}{(\Theta - 1)} \equiv F_{ncp,h} \tag{12}$$

The mean free path of gas molecules is connected with thermal conductivity coefficient k and other gas parameters by the monatomic gas equation

$$l_g = \frac{4}{5} \frac{k(T_g) T_g}{p_g} \sqrt{\frac{m_g}{2k_B T_g}} \tag{13}$$

where p_g is the equilibrium gas pressure. With account for this definition in the case of power law dependence (10), the ratio of the heat transfer rates calculated for continuum (7) and free-molecular regime (5) can be expressed:

$$\frac{\dot{q}_c}{\dot{q}_f} = \frac{5\sqrt{\pi}\, Kn}{\alpha} \frac{(\gamma^* - 1)}{(\gamma^* + 1)} \frac{\dot{q}_c}{\dot{q}_{c,1}} \tag{14}$$

Both the Knudsen number $Kn = l_g/a$ and the mean free path l_g are defined based on the unperturbed parameters of the background gas.

3. Interpolation formulae

There is no general analytical solution of the Boltzmann equation describing gas behavior in the intermediate regime of moderate Knudsen numbers, even in the case of small temperature differences. The use of interpolation formulae, verified by comparison with available numerical solutions or experimental data, appears to be the only feasible opportunity to predict particle–gas energy exchange in such a case.

[1] Lee [17], Lee et al. [6] and Chyou [18] have applied a similar model to calculate ion diffusion and heat fluxes to particles carried by plasma. However, they placed the limiting sphere about a few Debye lengths from the sphere, which is substantially shorter than the ion-neutral mean free path. This led to systematic errors in the range of large Knudsen numbers, as discussed by Leveroni and Pfender [19].

3.1. Fuchs' approach

Fuchs [15,16] proposed a general method to estimate the mass/energy transfer between the gas phase and isolated particle in cases when the particle size is comparable to the mean free path of the molecules under consideration in the gas. The method is based on the separation of the whole space outside the particle into two parts: the region outside the limiting sphere with radius $\delta + a$, concentric to the particle, and the boundary layer with thickness δ adjacent to the particle surface. The thickness of the boundary layer is chosen to be about the gas mean free path, and the molecular motion inside that layer considered as collisionless, while in the outer region the temperature distribution is described by means of continuum theory.[1]

Following Fuchs [15], we assume the definition of Wright [20] for the limiting sphere radius:

$$\frac{\delta + a}{a} = \frac{a^2}{l_\delta^2}\left(\frac{1}{5}\Lambda_1^5 - \frac{1}{3}\Lambda_2\Lambda_1^3 + \frac{2}{15}\Lambda_2^{5/2}\right) \tag{15}$$

The radius $\delta + a$ has a geometrical meaning of the average distance between the particle center and the points, lying in the gas one molecular mean free path l_δ away from some point on the particle surface:

$$\Lambda_1 = 1 + \frac{l_\delta}{a}; \quad \Lambda_2 = 1 + \left(\frac{l_\delta}{a}\right)^2 \tag{16}$$

In the case of large temperature ratios, the mean free path of molecules near the limiting sphere l_δ differs from the mean free path l_g far from the particle. The definition (13) of the mean free path yields

$$l_\delta = \frac{k(T_\delta)}{k(T_g)}\left(\frac{T_g}{T_\delta}\right)^{1/2} \cdot \frac{p_g}{p_\delta} l_g \tag{17}$$

Neglecting the effect of thermal stresses [21] in this approximate calculation, the pressures p_δ and p_g may be assumed equal. Then, in the case of power law (10), Eq. (17) yields

$$\frac{l_\delta}{a} = Kn\left(\frac{T_\delta}{T_g}\right)^{\omega+1/2} \tag{18}$$

If the molecular velocity distribution at the limiting sphere can be approximated as Maxwellian, the heat transfer rate from the particle can be calculated similarly to Eqs. (4) and (5):

$$\dot{q} = \alpha\pi a^2 \frac{p_g}{2}\sqrt{\frac{8k_B T_\delta}{\pi m_g}} \frac{\gamma^* + 1}{\gamma^* - 1}\left(\frac{T_p}{T_\delta} - 1\right) \tag{19}$$

where T_δ is the gas temperature at the limiting sphere and γ^* is the mean value of the adiabatic constant

obtained by averaging (6) with substitution $T_g \to T_\delta$ for the lower integration limit.

In the region outside the limiting sphere the continuum theory equations are assumed. Then, in the case of the power law dependence (10) for the heat conductivity the total heat flux is

$$\dot{q} = \frac{4\pi(\delta + a)k(T_g)T_g}{\omega + 1}\left[\left(\frac{T_\delta}{T_g}\right)^{\omega+1} - 1\right] \tag{20}$$

Since there are no sinks or sources of heat inside the δ-layer adjacent to the particle, Eqs. (19) and (20) in a quasi-stationary case describe the same physical quantity $\dot{q}$. Equating these formulae results in the following algebraic equation for T_δ:

$$\frac{5\sqrt{\pi}Kn}{\alpha(\omega + 1)}\left(1 + \frac{\delta}{a}\right)\frac{(\gamma^* - 1)}{(\gamma^* + 1)}\left[\left(\frac{T_\delta}{T_g}\right)^{\omega+1} - 1\right] = \left(\frac{T_p}{T_\delta} - 1\right)\cdot\sqrt{\frac{T_\delta}{T_g}} \tag{21}$$

where the ratio δ/a is a function of the temperature ratio T_δ/T_g, given by Eqs. (15), (16) and (18). This equation can be solved numerically to find the temperature T_δ. Then the heat transfer rate $\dot{q}$ can be calculated from Eq. (19).

3.2. Sherman and Fuchs–Loyalka interpolation formulae

Sherman [22] has found that in many experiments in the intermediate Knudsen regime, the rates of heat (or mass) transfer between a particle and a gas can be described by a simple algebraic formula of the harmonic mean form:

$$\frac{\dot{q}}{\dot{q}_c} = \left(1 + \frac{\dot{q}_c}{\dot{q}_f}\right)^{-1} \tag{22}$$

where the indices 'f' and 'c' denote the heat transfer rates in free-molecular and continuum regimes. Since the ratio q_c/q_f is proportional to the Knudsen number [see Eq. (14)], the structure of this formula guarantees correct limiting values q_c and q_f for the heat transfer rate in the continuum and free-molecular regimes, respectively.

Fuchs and Sutugin [23] and later Loyalka [24,25] have generalized the Sherman equation to the form:

$$\frac{\dot{q}}{\dot{q}_c} = \left(1 + Kn\frac{\xi\dot{q}_c/\dot{q}_f + \zeta}{\xi\, Kn + 1}\right)^{-1} \tag{23}$$

where ξ and ζ are dimensionless coefficients of order unity. Eq. (23) is written for the case of complete thermal accommodation ($\alpha = 1$).

For the cases when the energy accommodation coefficient α differs from unity, Cercignani and Pagani [26] introduced the following interpolation formula:

$$\frac{\dot{q}(\alpha)}{\dot{q}_c} = \frac{\dot{q}(1)}{\dot{q}_c}\left[1 + \frac{(1 - \alpha)}{\alpha}\frac{\dot{q}(1)}{\dot{q}_f(1)}\right]^{-1} \tag{24}$$

where the heat transfer rates $\dot{q}_f(1)$ and $\dot{q}(1)$ are given by Eq. (4) with $\alpha = 1$ and by Eq. (23), respectively.

Despite the fact that the detailed asymptotics of Eq. (23) in the free-molecular limit does not agree with more accurate results based on linearization of the BGK model equation (as shown by Tompson and Loyalka [27]), this interpolation formula describes known experimental results on heat transfer with excellent accuracy, provided the particle/gas temperature difference is small.

4. Direct Monte Carlo simulation

The discussed interpolation formulae are unlikely to be equally successful when $\Delta T/T_g$ is not small. In view of lack of experimental data on heat transfer under the considered highly non-equilibrium conditions, the numerical simulation appears to be the only possible tool for their verification.

Bird [7] has developed an effective technique called Direct Monte Carlo Simulation (DSMC), which has already been employed in a variety of highly non-equilibrium situations ranging from calculation of hypersonic rarefied flows [28] to creeping flows with very low Mach and Reynolds numbers caused by high temperature gradients at the channel walls [8]. We have invoked the Direct Monte Carlo Simulation (DSMC) technique to provide 'exact' solutions (of the Boltzmann equation) against which the performance of suitably generalized interpolation methods can be checked. For numerical tests, we have chosen a well-defined and simple hard sphere model, for which the heat conductivity coefficient is a function of temperature, described by the power law (10) with $\omega = 1/2$. The energy of the hard sphere molecules is connected only with their translation motion, so that value of the gas constant γ is 5/3 [10]. The hard sphere gas is a classical model for a DSMC simulation.

The space outside the spherical particle was divided into two parts, analogously to Fuchs' approach: in the outer region outside the limiting sphere with radius $\delta + a$, where the continuum theory equations are valid, and the layer adjacent to the particle with thickness δ, where the DSMC method is applied. However, in contrast to the Fuchs calculation, the width δ is chosen here to be large compared to the mean free path.

A general description of the DSMC method, including a considered case of spherical symmetry, is given in a book of Bird [7]. In our calculations, billions of gas

molecules were represented computationally by 4×10^5 simulated molecules. The δ-layer was divided into 200 concentric shells of equal thickness. All calculations started from an initial state of isothermal gas. Velocity components and position coordinates of the molecules were stored and modified with the time as the molecules undergo collisions and boundary interactions in simulated physical space. Inter-molecular collisions were simulated using the classical model for hard spheres. The collisions between the molecules and the particle surface are, in the general case, described by the following equation for the velocity distribution function of molecules f:

$$f(\boldsymbol{v}) = \int_{\boldsymbol{v}'\boldsymbol{n}<0} R(\boldsymbol{v}', \boldsymbol{v}) f(\boldsymbol{v}') \mathrm{d}\boldsymbol{v}'; \quad \boldsymbol{v}\boldsymbol{n} > 0 \tag{25}$$

where $\boldsymbol{v}'$ and $\boldsymbol{v}$ are the velocities of the incident and reflected molecules and $\boldsymbol{n}$ is the external normal to the particle surface and R is the scattering kernel function.

To account for momentum and energy accommodation of molecules on the particle surface, the scattering process was simulated as a simple combination of specular reflection and completely diffuse reflection (Maxwell model) with the following scattering kernel:

$$R(\boldsymbol{v}', \boldsymbol{v}) = (1-\alpha)\delta_{\mathrm{D}}(\boldsymbol{v}' - \boldsymbol{v} + 2\boldsymbol{n}[\boldsymbol{n}\boldsymbol{v}]) + \alpha f_0(\boldsymbol{v}, T_{\mathrm{p}}) \mid \boldsymbol{v}\boldsymbol{n} \mid \tag{26}$$

$$f_0(\boldsymbol{v}, T_{\mathrm{p}}) = \left(\frac{m}{2\pi k T_{\mathrm{p}}}\right)^{3/2} \cdot \exp\left(-\frac{m\boldsymbol{v}^2}{2kT_{\mathrm{p}}}\right) \tag{27}$$

where δ_{D} is the Dirac delta function and f_0 is the Maxwellian equilibrium velocity distribution.

On the opposite boundary $r = \delta + a$ the molecules leaving the computational volume were instantly substituted by the incoming molecules with velocity distribution, calculated with account for the first correction to the equilibrium distribution in the presence of the radial temperature gradient [29]:

$$f(v) = f_0(v, T_\delta)\left[1 - \frac{2}{5}\sqrt{\frac{2m_{\mathrm{g}}}{k_{\mathrm{B}}T_\delta}}\frac{k(T_\delta)}{n_\delta k_{\mathrm{B}} T_\delta} v_{*\mathrm{r}}\left(v_*^2 - \frac{5}{2}\right)\frac{\mathrm{d}T_\delta}{\mathrm{d}r}\right] \tag{28}$$

$$\boldsymbol{v}_* = \sqrt{\frac{m_{\mathrm{g}}}{2k_{\mathrm{B}}T_\delta}}\boldsymbol{v} \tag{29}$$

where $\boldsymbol{v}_*$ is a dimensionless molecular velocity and $v_{*\mathrm{r}}$ is its radial component. The molecule concentration n_δ at the limiting sphere can be expressed in terms of T_δ using

$$n_{\mathrm{g}} k_{\mathrm{B}} T_{\mathrm{g}} = n_\delta k_{\mathrm{B}} T_\delta - \frac{4}{5} k(T_\delta)\sqrt{\frac{m_{\mathrm{g}}}{2\pi k_{\mathrm{B}} T_\delta}}\frac{\mathrm{d}T_\delta}{\mathrm{d}r} \tag{30}$$

which is the condition of gas equilibrium (see, e.g., [7]). The second term on the right-hand-side of Eq. (29) is a contribution of the thermal stress to the gas pressure at the limiting sphere, which was neglected in the Fuchs model [cf. Eqs. (17) and (18)].

The distance δ in calculations was chosen large enough to ensure the applicability of continuum transport equations in the outer region $r > \delta + a$, and to guarantee the smallness of the terms proportional to the temperature gradients in Eqs. (28) and (30) so that the higher-order corrections could be neglected:

$$\delta = 5(l_{\mathrm{g}} + a), \quad Kn < 5$$

$$\delta = 2l_{\mathrm{g}}, \quad Kn \geq 5 \tag{31}$$

Because the temperature T_δ is a priori unknown, the DSMC problem is not closed and the numerical solution must be matched with the continuum solution in the outer region. This is implemented iteratively. Initially, some guess value is taken for T_δ. According to Eq. (20), this yields a guess for the heat flow $\dot{q}$. Then the value of the temperature gradient at the limiting sphere can be obtained from

$$\frac{\mathrm{d}T_\delta}{\mathrm{d}r} = -\frac{\dot{q}}{4\pi(\delta + a)^2 k(T_\delta)} \tag{32}$$

Thus, all parameters of the velocity distribution (28) are fixed and the following step of the DSMC calculation can be performed, including both collision and free-streaming stages to update the velocities and molecule positions. After this, since the internal energy and the heat flow in a hard sphere gas are connected only with translation motion of the molecules, a new value of the total heat flow can be calculated in the δ-layer:

$$\dot{q} = 4\pi r^2 \left\langle \frac{m}{2} v_{\mathrm{r}} v^2 \right\rangle \tag{33}$$

where the brackets denote the averaging in the velocity space. The procedure of averaging (33) in the DSMC method is substituted by taking the average over the calculation cell (shell in our case). In a stationary case, the integral flux (33) does not depend on the radial coordinate r, and the spatial averaging over the interval $a < r < \delta + a$ was performed to reduce the statistical noise.

Based on obtained quantities $\dot{q}$, the values of the temperature and the temperature gradient at the limiting sphere are calculated, and the next iteration follows. To stabilize the convergence process, the average value of q calculated at many preceding steps was

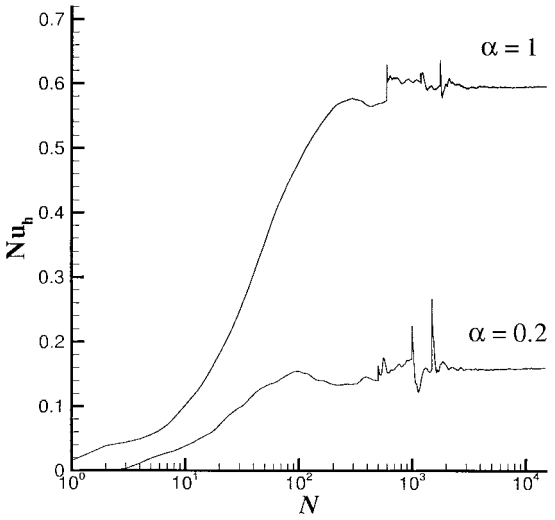

Fig. 1. The Nusselt number as a function of the time step number N calculated for $Kn = 1$, $\Theta = 10$ and two values of the accommodation coefficient $\alpha = 1$ and $\alpha = 0.2$.

used. At points $N = N_1$, N_2, N_3 (where $N_1 \approx 500$, $N_2 = 2 \times N_1$ and $N_3 = 3 \times N_1$) the time averaging started anew (to let the system completely 'forget' the initial conditions), so that for some time step N_c with $N_c > N_3$ the value of q was taken as the time average of all those calculated [by spatial and ensemble averaging (33)] in the interval $N_3 < N < N_c$. The time step was chosen to be less than 5% of the average time between intermolecular collisions.

Such a procedure yielded good convergence shown in Fig. 1 for $\Theta = 10$, $Kn = 1$ and two values of accommodation coefficient $\alpha = 0.2$ and $\alpha = 1$. The Nusselt number Nu_h is defined by

$$Nu_h \equiv \frac{\dot{q}}{2\pi a k(T_g)(T_p - T_g)} \tag{34}$$

where the reference heat transfer rate is the constant property value. At points $N_1 \approx 500$, $N_2 = 1000$ and $N_3 = 1500$ the averaging over preceding time steps started anew, which resulted in instant fluctuations of Nu_h. A relatively good accuracy of solution can be reached already after about 5000 time steps, and a minimal number of time steps in our calculations was 15,000.

5. Results and discussion

5.1. Comparison of DSMC with interpolation formulae

The described DSMC method can provide detailed information about the gas parameters near the particle over a rather wide range of temperature ratio Θ.

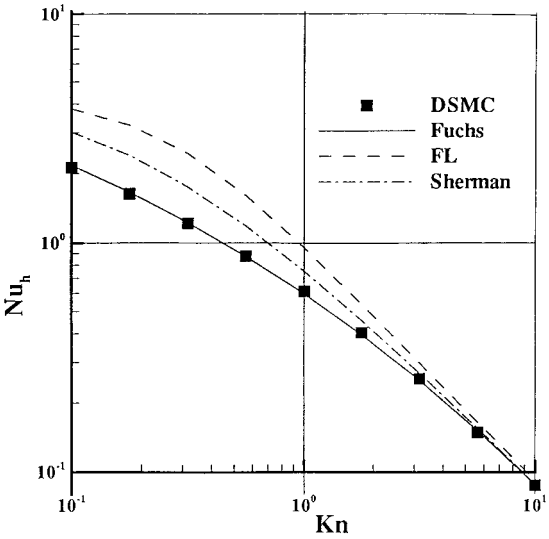

Fig. 2. Nusselt numbers for high temperature ratio $\Theta = 10$ in the case of complete accommodation. Shown are the calculated results (squares) and values given by the variable property extension of the Fuchs theory, Sherman and Fuchs–Loyalka formulae.

However, the primary goal of the calculations was to find the values of heat transfer rate q and compare them with predictions of the discussed interpolation formulae.

The calculated Nusselt numbers, determined for two values of the accommodation coefficients $\alpha = 1$ and $\alpha = 0.3$ are shown in Figs. 2 and 3, respectively. The results of the DSMC calculations are shown by squares.

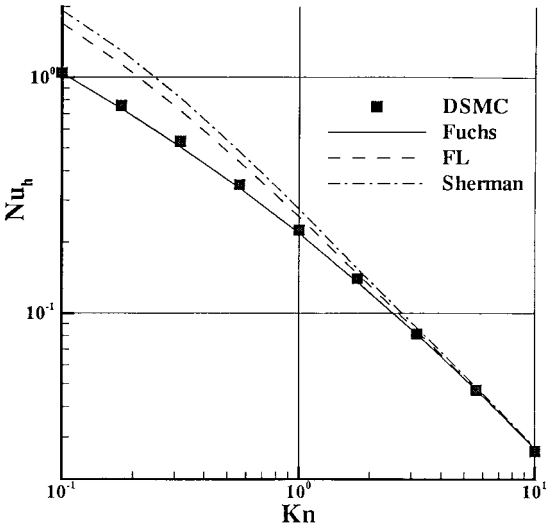

Fig. 3. Nusselt numbers calculated for the temperature ratio $\Theta = 10$ and accommodation coefficient $\alpha = 0.3$.

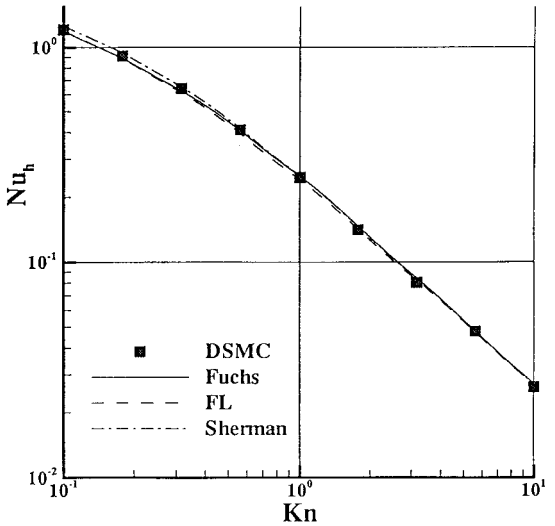

Fig. 4. Nusselt numbers in the case of small particle/gas temperature difference with $\Theta = 1.3$ and accommodation coefficient $\alpha = 0.3$.

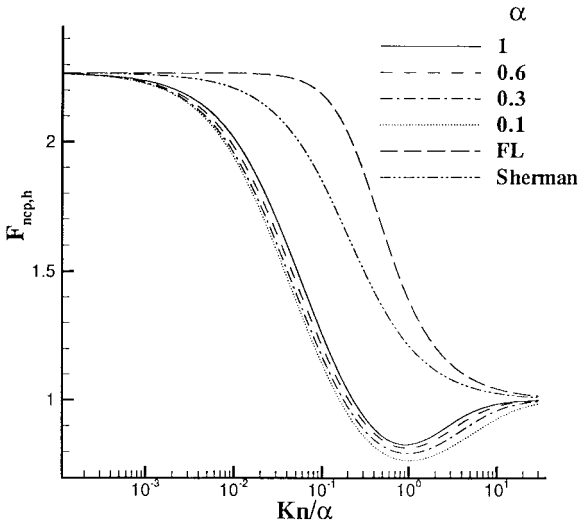

Fig. 5. Non-constant property correction factor as a function of the ratio of the Knudsen number to the accommodation coefficient for $\Theta = 10$ (variable property extension of the Fuchs theory) for different values of accommodation coefficient. Also shown are the results predicted by the Sherman formula and by the Fuchs–Loyalka formula for $\alpha = 1$ and the same value of Θ.

The results predicted by the Fuchs–Loyalka formulae (23) and (24) with $\zeta = 1.3026$ and $\xi = 1.9234$ (dashed line) and by the Sherman formula (22) (dashed–dotted line) overestimate the heat exchange rates and do not agree with DSMC. On the contrary, the predictions of the generalized Fuchs theory (solid line) appear to hold well at all values of the temperature ratio and the accommodation coefficient and do not require corrections depending on the nature of the gas.

As a test, the Nusselt numbers have been determined for relatively close particle and gas temperatures with a ratio $\Theta = 1.3$ in the case $\alpha = 0.3$. The results obtained using different methods in these cases are shown in Fig. 4 and agree remarkably well. Increasing the level of the statistical level presents the use of the DSMC model for particle/gas temperature differences with $|\Theta - 1| < 0.3$. However, this case is already very well studied, both experimentally and theoretically.

In general, the comparison of the DSMC predictions with results based on different interpolation formulae has shown that the generalized Fuchs model describes the heat transfer rates at various temperature ratios and Knudsen numbers most accurately, which makes it preferable to use in various applications, including LII analysis.

5.2. Non-constant property correction factor for different interpolation formulae

To characterize the deviation from the low temperature difference solution, it is convenient to introduce the non-constant property correction factor $F_{\mathrm{ncp,h}}$ as the ratio of two Nusselt numbers:

$$F_{\mathrm{ncp,\,h}} \equiv \frac{Nu_{\mathrm{h}}(\Theta)}{Nu_{\mathrm{h}}(1)} \tag{35}$$

where the denominator is the limiting value of the function (34) at $T_{\mathrm{p}} \to T_{\mathrm{g}}$, and all other parameters are the same for both Nusselt numbers.

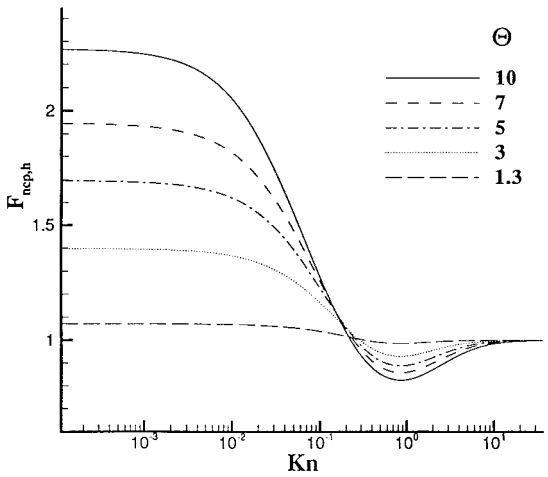

Fig. 6. Dependencies of the non-constant property correction factor on the Knudsen number for different temperature ratios in the case of complete accommodation, calculated using the variable property extension of the Fuchs model.

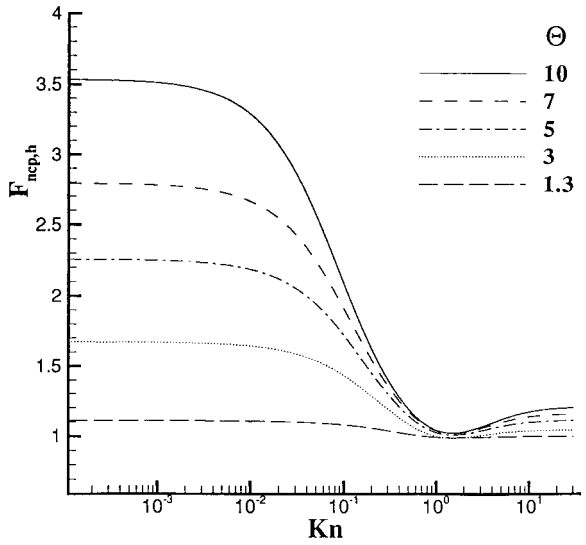

Fig. 7. Non-constant property correction factor for nitrogen. The background gas temperature $T_g = 300$ K and complete accommodation on the particle surface are assumed (Fuchs model).

In the continuum limit $Kn \to 0$ the denominator of the Eq. (35) equals 2, so that the correction factor $F_{ncp,h}$ coincides with the ratio of non-linear and linear heat transfer rates given by Eq. (12) for the case of power law dependence of the heat conductivity coefficient. In the free-molecular limit, formula (4) yields the following equation:

$$F_{ncp,\,h} = \frac{(\gamma^* + 1)(\gamma - 1)}{(\gamma^* - 1)(\gamma + 1)} \tag{36}$$

where γ^* is the average value of the adiabatic constant defined by Eq. (6), while γ is its value at $T = T_g$. For monatomic gases in the free-molecular limit the correction factor $F_{ncp,h}$ equals unity.

Figs. 5–7 show the dependencies of the correction factor on the Knudsen number in the intermediate regime for monatomic gas of hard spheres with $\omega = 1/2$ and $\gamma = 5/3$. Most of the data are obtained using the generalized Fuchs two-layer model, which agrees excellently with the DSMC model at high temperature ratios, but remains applicable also when the particle/gas temperature difference is small. The latter quality is necessary to calculate the denominator $Nu_h(1)$ in Eq. (35). The dependencies reach maxima in the continuum limit and have minima in the region of moderate Knudsen numbers, with positions depending mainly on the accommodation coefficient α (Fig. 5). It is interesting to observe that if the values of the correction factor are plotted against the ratio Kn/α, the curves appear to be very close, differing only up to about 10%. Remarkably, neither of two alternative interpolation formulae (20) and (21) predicts minima for the factor $F_{ncp,h}$ in the range of intermediate Knudsen numbers. This non-monotonic behavior is connected with non-linear dependence of the real heat flow rates from the particle in the transition regime, which are lower, than could be expected based on simple interpolations between the continuum and free-molecular values.

A variation of the temperature ratio Θ at a fixed value of accommodation coefficient ($\alpha = 1$) results in an increase of the continuum limit value of the correction factor and in a decrease of its minimum value (Fig. 6). For real gases, this picture may be different (Fig. 7). Here, the correction factor is calculated for molecular nitrogen with background temperature $T_g = 300$ K at various particle/gas temperature ratios and complete accommodation at the particle surface. The exponent for the temperature dependence of the heat conductivity coefficient was set to $\omega = 0.76$ [30], while the values for adiabatic constant γ in the interval $300\ \text{K} \le T \le 3000\ \text{K}$ were taken from the JANAF tables [13]. Although the minima of the curves with positions almost independent on Θ are also observed (cf. Fig. 6), the limiting values of the correction factor in the free-molecular limit are all different due to variation of γ with temperature.

5.3. Applicability of results to transient heat transfer problems

In LII aerosol particle heat-up, as well as in some other applications, the particle temperature may change very rapidly due to various energy transfer mechanisms. The free-molecular heat transfer law (19) is based only on the assumption of Maxwellian gas molecule velocity distribution far (at 'infinity') from the particle and an energy accommodation model for molecule–surface interaction. If these assumptions are applicable, Eq. (19) is valid for any rate of particle heat-up/cooling.

However, in the transition and continuum regimes, the quasi-stationary approach of this paper can be used only if the characteristic time for particle cooling or heat-up, $\tau_{p,h}$, is substantially larger than the characteristic time τ_{eq} for equilibration of the molecular distribution near the particle.

In the continuum regime the relevant equilibration time can be calculated as the time necessary for a thermal 'wave' to propagate the distance a:

$$\tau_{eq} \equiv \frac{a^2 \rho_g c_v}{k(T_g)}, \quad Kn \ll 1 \tag{37}$$

while in the transition regime (Kn of order unity) it can be estimated as the ratio of the particle size to the characteristic molecular thermal velocity (which fol-

lows from the structure of the Boltzmann equation):

$$\tau_{eq} \equiv \frac{a}{\bar{c}}, \quad Kn = O(1) \tag{38}$$

where c_v is gas specific heat capacity. In calculating the cooling time, consider, for example, the case when a particle changes its temperature only due to heat transfer to the carrier gas. Then, according to Eqs. (7) and (19) (Fuchs model) for the heat transfer rates, we have the following estimates for characteristic cooling time τ_{ch} in the continuum and transition regimes:

$$\tau_{p,\,h} \equiv \frac{a^2 \rho_p c_p}{3k(T_g)}, \quad Kn \ll 1 \tag{39}$$

where c_p is the specific heat capacity of the particle.

Eqs. (37)–(40) yield the following conditions of applicability of the quasi-stationary approach:

$$\tau_{p,\,h} = \frac{2m_p c_p}{\alpha \pi a^2 p_g \bar{c}}, \quad Kn = O(1) \tag{40}$$

$$\frac{\tau_{p,\,h}}{\tau_{eq}} = \frac{\rho_p c_p}{\rho_g c_v} \gg 1, \quad Kn \ll 1 \tag{41}$$

$$\frac{\tau_{p,\,h}}{\tau_{eq}} = \frac{\rho_p c_p m_g}{\alpha \rho_g k_B} \gg 1, \quad Kn = O(1) \tag{42}$$

Conditions (41) and (42) always hold due to much higher density of the particle compared to the gas density ρ_g, while the particle and gas specific heat capacities and the gas constant k_B/m_g are of the same order-of-magnitude. Therefore, the quasi-steady approach is typically applicable to dense spherical particles and aggregates.

However, this is not necessarily the case for sparse aggregates, consisting, for example, of many dense spherules of comparable size a_0. In the free-molecule regime, the quasi-steady approach to calculation of the aggregate/gas heat transfer is applicable on the same conditions (Maxwellian molecule velocity distribution at infinity and energy accommodation model) as for a single particle. Due to weak thermal 'shielding' [31], the free-molecular heat transfer rate from each spherule in a sparse aggregate is comparable to the heat transfer rate (5) from an isolated single spherule at the same temperature.

The heat transfer from the particle aggregate in the continuum regime is the same as from a sphere with the equivalent radius R_{eq}, which coincides with the equivalent diffusion radius and the electrical capacitance of the aggregate [32]. Therefore, instead of condition (42) we have the following one:

$$\frac{\tau_{p,\,h}}{\tau_{eq}} \equiv \frac{\rho_p c_p}{\rho_g c_v} \frac{a_0^3 N}{3 R_{eq} L^2} \gg 1, \quad \frac{l_g}{L} \ll 1 \tag{43}$$

where L is the geometric diameter of the aggregate. In the transition regime, consider a Fuchs' δ-layer with a thickness of about a mean free path around the aggregate, inside which the inter-molecular collisions are negligible. Repeating the considerations made for a single particle, we arrive at the following condition:

$$\frac{\tau_{p,\,h}}{\tau_{eq}} \equiv \frac{\rho_p c_p m_g}{\rho_g k_B} \frac{a_0}{L} \gg 1, \quad \frac{l_g}{L} = O(1) \tag{44}$$

Since the spherule radius a_0 is always smaller than the equivalent radius R_{eq} and the aggregate size L, satisfaction of condition (43) guarantees the applicability of the quasi-steady approach, not only in the continuum regime, but also in the transition regime [Eq. (44)]. These conditions do not follow from conditions (41) and (42) and must be checked before applying formulas based on discussed quasi-steady analysis, especially for large aggregates at high pressure.

5.4. Other energy transfer mechanisms

Depending on the particle and gas temperature, there can be a variety of energy transfer mechanisms, acting simultaneously with ordinary molecular heat transfer treated here. For example, the particle material may evaporate, thus creating a sink of energy, which often becomes a dominating cooling mechanism for hot particles above some critical temperature. Also, the particle surface, heated up to several thousand Kelvins, may cause dissociation of the incident polyatomic gas molecules, thus increasing the heat loss rate. At very high temperatures and for relatively large particles, the radiation losses can also become non-negligible. When these processes dominate the particle cooling, the associated cooling times are substantially smaller than the characteristic time due to background gas heat conductivity [Eqs. (39) and (40)]. Then, if the ratio of the cooling time to the equilibration time (37) and (38) is comparable to or smaller than unity, the quasi-steady heat transfer rates, calculated in this paper, become less accurate. However, if the contribution of other mechanisms to the total energy transfer is overwhelming, the exact calculation of the heat conductivity from the particle loses importance.

These alternative energy transport mechanisms must be considered to correctly model the evolution of the particle temperature under highly non-equilibrium conditions, as in the case of LII measurement or plasma processing, and will be discussed in a follow-up paper. It should also be said that while, for the purpose at hand, we simply specified constant values of the physical parameter α (<1), representing the overall energy

accommodation coefficient for molecular encounters with the hot solid surface, in practice the actual shape of the Knudsen transition could be more complicated (cf. Fig. 7) if this coefficient had a substantial dependence on the temperatures T_p and/or T_g. For any particular gas/solid combination this kind of dependence is not uncommon (see Refs. [9] and [12]), although such data are often not readily available for the systems of great engineering interest.

6. Conclusions

Heat transfer rates between a highly 'overheated' spherical particle and its carrier gas have been calculated using a direct simulation Monte-Carlo (DSMC-) technique over a wide range of Knudsen numbers. Our quasi-steady results for the test case of a hard sphere monatomic ideal gas, and at absolute temperature ratios T_p/T_g up to 10, were compared with predictions of two available interpolation formulae and the 'two-layer-in series' model of Fuchs, suitably generalized to incorporate variable thermophysical properties. The DSMC results, considered here to be 'exact' representations of the non-equilibrium Boltzmann equation solution, are found to be conveniently described by the variable property extension of the Fuchs model, making it our recommended method for rapid calculations of particle/gas heat transfer rates in the Knudsen transition regime at large particle/gas temperature ratios. This information is necessary (if not sufficient) in a number of applications, including the interpretation of laser-induced incandescence (LII-) signals to infer accurate aerosol particle size distributions [33]. We note that sublimation and/or dissociation effects, beyond the scope of the present contribution, will also have to be taken into account in many applications of LII.

It is interesting to observe (see Figs. 6–9) that the variable property correction at any particular T_p/T_g significantly larger than unity is not monotonic in the Knudsen number, causing simple interpolation schemes (between the free-molecule and continuum limits) to fail rather badly. We conclude that the equations developed here can be used for the case of highly overheated spheres in polyatomic ideal gases with arbitrary temperature-dependent heat capacity and thermal conductivity. Moreover, while explicitly derived for the case of a solid spherical particle, these variable property correction equations/results are expected to be particle shape/morphology insensitive.

Acknowledgements

This research was supported by Grants AFOSR F49620-97-0266 and NASA NAG 3-1951.

References

[1] L. Lees, Kinetic theory description of rarefied gas flow, J. Soc. Ind. Appl. Math. 13 (1965) 278–311.
[2] M.M.R. Williams, S.K. Loyalka, Aerosol Science: Theory and Practice, Pergamon Press, New York, 1991.
[3] P. Roth, A.V. Filippov, In situ ultrafine particle sizing by a combination of pulsed laser heatup and particle thermal emission, J. Aerosol Sci. 27 (1996) 95–104.
[4] R.L. Vander Wal, K.J. Weiland, Laser-induced incandescence: development and characterization towards a measurement of soot-volume fraction, Appl. Phys. B59 (1994) 445–452.
[5] C. Xi, H. Ping, Heat transfer from a rarefied plasma flow to a metallic or nonmetallic particle, Plasma Chem. Plasma Process. 6 (1986) 313–333.
[6] Y.C. Lee, Y.P. Chyou, E. Pfender, Particle dynamics and particle heat and mass transfer in thermal plasmas. Part II: Particle heat and mass transfer in thermal plasmas, Plasma Chem. Plasma Process. 5 (1985) 391–416.
[7] G.A. Bird, Molecular Gas Dynamics and the Direct Simulation of Gas Flows, Clarendon Press, Oxford, 1994.
[8] D.H. Papadopoulos, D.E. Rosner, Enclosure gas flows driven by non-isothermal walls, Phys. Fluids 7 (1995) 2535–2537.
[9] D.E. Rosner, D.H. Papadopoulos, Jump, slip and creep boundary conditions at non-equilibrium gas/solid interfaces, I/EC-Research (ACS) 35 (9) (1996) 3210–3222.
[10] E.H. Kennard, Kinetic Theory of Gases, McGraw-Hill, New York, 1938.
[11] G.M. Hidy, J.R. Brock, The Dynamics of Aerocolloidal Systems, Pergamon Press, New York, 1970.
[12] J.R. Burke, D.J. Hollenbach, The gas–grain interaction in the interstellar medium: thermal accommodation and trapping, Astrophys. J. 265 (1982) 223–234.
[13] JANAF Thermodynamical Tables, 1985, 3rd ed., J. Phys. Chem. Ref. Data, 14 (Suppl. 1).
[14] D.E. Rosner, Transport Processes in Chemically Reacting Flow Systems, Butterworth-Heinemann, Stoneham, MA, 1986 (Dover Publications, in press).
[15] N.A. Fuchs, On the stationary charge distribution on aerosol particles in a bipolar ionic atmosphere, Geophys. Pura Appl. 56 (1963) 185–193.
[16] N.A. Fuchs, The Mechanics of Aerosols, Pergamon Press, Oxford, 1964 (Dover Publications, New York, 1989).
[17] Y.C. Lee, Modeling work in thermal plasma processing, Ph.D. dissertation, University of Minnesota, MN, 1984.
[18] Y.P. Chyou, Modeling of thermal plasma processing, Ph.D. dissertation, University of Minnesota, MN, 1987.
[19] E. Leveroni, E. Pfender, A unified approach to plasma–particle heat transfer under non-continuum and non-equilibrium conditions, Int. J. Heat Mass Transfer 29 (1990) 1497–1509.
[20] P.G. Wright, On the discontinuity involved in diffusion across an interface (the Δ of Fuchs), Discuss. Faraday Society 30 (1960) 100–112.
[21] D.W. Mackowski, D.H. Papadopoulos, Comparison of Burnett and DSMC predictions of pressure distributions

and normal stress in one-dimensional non-isothermal gases, Phys. Fluids A 1999 (in press).
[22] F.S. Sherman, A survey of experimental results and methods for the transition regime of rarefied gas dynamics, Proceedings of the Third International Symposium on Rarefied Gas Dynamics II (1963) 228–260.
[23] N.A. Fuchs, A.G. Sutugin, Highly Dispersed Aerosols, Ann Arbor Science, Ann Arbor, 1970.
[24] S.K. Loyalka, Condensation on a spherical droplet, J. Colloid Interface Sci. 87 (1981) 216–224.
[25] S.K. Loyalka, Mechanics of aerosols in nuclear reactor safety: a review, Progress in Nuclear Energy 12 (1983) 1–56.
[26] C. Cercignani, C.D. Pagani, Variational approach to rarefied flows in cylindrical and spherical geometry, Proceedings of the Sixth International Symposium on Rarefied Gas Dynamics II (1964) 555–573.
[27] R.V. Tompson, S.K. Loyalka, Condensational growth of a spherical droplet: free molecular limit, J. Aerosol Sci. 17 (1986) 723–728.
[28] V.K. Dogra, J.N. Moss, R.G. Wilmoth, J.M. Price, Hypersonic rarefied flow past spheres including wake structure, J. Spacecraft and Rockets (AIAA) 31 (1994) 713–718.
[29] S. Chapman, T.G. Cowling, The Mathematical Theory of Non-Uniform Gases, 3rd ed., Cambridge University Press, 1991.
[30] R.A. Svehla, Estimated viscosities and thermal conductivities of gases at high temperatures, Technical Report No. R-132, NASA, Washington, DC, 1962.
[31] A. Schmidt-Ott, U. Baltensperger, H.W. Gaggeler, J.T. Jost, Scaling behavior of physical parameters describing agglomerates, J. Aerosol Sci. 21 (1990) 711–717.
[32] A.V. Filippov, Charge distribution along non-spherical particles in a bipolar ion environment, J. Aerosol Sci. 25 (1994) 611–615.
[33] A.V. Filippov, D.E. Rosner, M. Kumar, When and how can time-resolved LII be used to extract aggregate size distributions, Comb. Sci. Technol. (in press).